

## BOUSSINESQ-TYPE MOMENTUM EQUATIONS SOLUTIONS FOR STEADY RAPIDLY VARIED FLOWS

Yebegaeshet T. Zerihun<sup>1</sup> and John D. Fenton<sup>2</sup>

### ABSTRACT

The depth averaged Saint-Venant equations are adequate in simulating free surface flows with insignificant curvature of streamlines. However, these equations are insufficient when applied to flow problems where the effects of non-hydrostatic pressure distribution are predominant. In this study, two Boussinesq-type momentum equation models are employed to simulate such types of flow problems numerically. Assumptions of uniform and linear variation of the centrifugal term with depth are used to develop the models. The effect of these assumptions on the solutions of the models is also assessed. Two numerical simulation case studies, flow over a short-crested trapezoidal profile weir and a free overfall, are considered. Computed and measured results for flow and bed pressure profiles, and pressure distributions at different sections are presented. Good agreement is attained between the computed and measured results. The comparison results suggest that the assumed distribution shapes for the centrifugal term strongly influences the prediction of the pressure profiles, but the effect is minor on the flow profile results.

### 1. INTRODUCTION

The streamlines in rapidly varied free surface flows have considerable curvatures and slopes. These cause a departure from hydrostatic pressure and uniform velocity distributions. In engineering practice, transcritical flow over hydraulic structures such as spillway and weirs are examples of flows having this kind of nature. The common computational flow models, which are based on the depth averaged Saint-Venant equations, cannot be used to simulate such types of flow problems. In the formulation of the Saint-Venant equations, assumptions of uniform velocity and hydrostatic pressure distributions are employed. These assumptions restrict the application of the equations to flow situations where the effects of non-hydrostatic pressure distribution are insignificant. The essential vertical flow details of the rapidly varied flow problems determine the use of relatively accurate methods for exact description of the flow situations.

Considerable researches have been done in the past to model free surface curved flow problems using different approaches. Boussinesq (1877) was the first to extend the momentum equation to incorporate implicitly the effect of curvature of the streamlines using the assumption of a linear variation of curvature of streamlines along the depth of flow. More recently Dressler (1978),

---

<sup>1</sup> Graduate Student, Department of Civil and Environmental Engineering, The University of Melbourne, Victoria 3010, Australia (y.zerihun@civenv.unimelb.edu.au)

<sup>2</sup> Professorial Fellow, Department of Civil and Environmental Engineering, The University of Melbourne, Victoria 3010, Australia (fenton@unimelb.edu.au)

Hager and Hutter (1984), Hager (1985) and Matthew (1991) have developed higher-order equations to model two-dimensional flow problems. Similar to the Boussinesq (1877) equation, however these equations are limited to the solution of irrotational flow problems only. For fast flow over the chute part of hydraulic structures such as spillways, the assumption of irrotational flow, which was the basis of all these governing equations, is questionable. It has also been shown by Fenton (1996) that the scaling of the variables introduced into the Dressler equations has an inconsistency. Steffler and Jin (1993) developed the vertically averaged and moment (VAM) equations based on the assumptions of a linear longitudinal velocity distribution, and quadratic pressure and vertical velocity distributions along the depth of flow. However, the resulting equations are very long and complex. Khan and Steffler (1996a, b) studied the applicability of these equations. Fenton (1996) introduced alternative equations to model flow problems with appreciable curvature of streamline. He used the momentum principle along with the assumption of a constant centrifugal term,  $\kappa/\cos\alpha$  ( $\kappa$  = curvature and  $\alpha$  = angle of inclination of the streamline with the horizontal axis), at a vertical section to develop the equations. The distribution shape of this term determines the degree of the approximation for the effects of the streamline curvature. Compared to other governing equations (for instance, Dressler and VAM equations), the equations are simple to apply in a cartesian coordinate system especially for flow problems with continuous flow boundaries. In this study, these equations along with the modified version, which are developed based on the assumption of a linear variation of centrifugal term along the flow depth, will be employed to simulate steady rapidly varied flows. These include transcritical flow over short-crested trapezoidal profile weirs and free overfall in a rectangular channel. The free overfall problem has been extensively studied numerically (e.g., Khan and Steffler (1996b)). Compared to this, however free flow over trapezoidal profile weirs has not been thoroughly investigated numerically using lower- or higher-order equation.

Therefore, the purposes of this paper are: i) to examine the Boussinesq-type equations models for simulating steady rapidly varied flows; and ii) to assess systematically the impact of the applied distribution shapes for the variation of the centrifugal term on the simulation of pressure and flow surface profiles of such flows.

## 2. GOVERNING EQUATIONS

For steady flow in a rectangular channel, the Boussinesq-type equations developed by Fenton (1996) read as

$$\frac{\beta q^2}{4} \frac{d^3 H}{dx^3} + \frac{\beta Z'_b q^2}{2H} \frac{d^2 H}{dx^2} + (1 + Z_b'^2) \left( \left( gH - \beta \frac{q^2}{H^2} \right) \frac{dH}{dx} + gH(Z_b' + S_f) \right) + \omega_0 \beta q^2 \left( \frac{Z_b'''}{2} + \frac{Z_b' Z_b''}{H} \right) = 0, \quad (1)$$

$$p = \rho(\eta - z) \left( g + \frac{\beta q^2}{H^2 (1 + Z_b'^2)} \left( \omega_0 Z_b'' + \frac{1}{2} \frac{d^2 H}{dx^2} \right) \right), \quad (2)$$

in which  $H$  is the depth of flow;  $Z_b'$ ,  $Z_b''$  and  $Z_b'''$  are the first, second and third derivatives of the bed profile respectively;  $S_f$  denotes the friction slope, calculated from the Manning equation or smooth boundary resistance law;  $q$  is the discharge per unit width;  $\beta$  refers to the Boussinesq coefficient;  $g$  is gravitational acceleration;  $\rho$  is the density of the fluid;  $\eta$  is elevation of the free surface;  $z$  is the vertical coordinate of a point in the flow field;  $p$  is the pressure; and  $\omega_0$  is a weighting factor. Fenton (1996) suggested a value of slightly less than one for  $\omega_0$ . These equations, eqs.1 and 2, will be referred to hereafter as the Boussinesq-type momentum equation of uniform

centrifugal term (BTMU) model. Following the procedures suggested by Fenton (1996) and assumptions of a linear variation of centrifugal term and average horizontal flow velocity, the following equations are developed for steady flow in a rectangular channel:

$$\frac{q^2}{3} \frac{d^3 H}{dx^3} + \frac{Z_b' q^2}{2H} \frac{d^2 H}{dx^2} + \left( gH - \beta \frac{q^2}{H^2} \right) \frac{dH}{dx} + gH(Z_b' + S_f) + q^2 \left( \frac{Z_b'''}{2} + \frac{Z_b' Z_b''}{H} \right) = 0, \quad (3)$$

$$p = \rho \left( g(\eta - z) + \frac{q^2}{H^2} \left( Z_b''(\eta - z) + \frac{d^2 H}{dx^2} \left( \frac{\eta - z}{\eta - Z_b} \right) \left( \frac{1}{2}(\eta + z) - Z_b \right) \right) \right). \quad (4)$$

These equations in this paper are termed the Boussinesq-type momentum equation linear (BTML) model. In the formulation of both models, the curvature at the surface is approximated by  $\kappa_H \cong d^2 H / dx^2 + Z_b''$  and at the bed by  $\kappa_b \cong Z_b''$ . If eq. 4 is compared with the corresponding equation, eq. 2, it is noticed that the term, which accounts for the dynamic effect due to the curvature of the flow surface, shows a quadratic variation in eq. 4. It should be remarked that eq. 2 predicts a linearly vary non-hydrostatic pressure distribution. In this work the two models will be applied to simulate flow in the vicinity of rectangular free overfall and flow over short-crested trapezoidal profile weirs. The numerical solution procedures for the latter flow problem are described in detail in the companion paper (Zerihun and Fenton (2004)) and only the simulation results are presented in this paper. A brief discussion of the modelling of the free overfall problem will be given in the following section. The simulation results of the two models will be compared with measurements to examine the influence of the applied distribution shapes for the variation of the centrifugal term on the solutions of the models.

### 3. DEVELOPMENT OF THE NUMERICAL MODEL AND SOLUTION

#### 3.1 Problem Formulation and Boundary Conditions

The computational domain for the numerical solution of the free overfall problem is shown in Figure 1. In this figure AB is the inflow section, EF is the outflow section and BD is the channel bed. The inflow section of the computational domain is located in a region where the flow is assumed to be nearly horizontal, with uniform velocity and hydrostatic pressure distributions. This flow condition simplifies the evaluation of the boundary values at this section using the gradually varied flow equation,

$$S_H = \frac{dH}{dx} = \frac{S_0 - S_f}{1 - \beta Fr^2}, \quad (5)$$

from which for the given depth and discharge at the inflow section, the corresponding slope of the water surface,  $S_H$ , can be evaluated numerically. In this equation,  $Fr$  is the Froude number and  $S_0$  is the bed slope. Besides, for the specified elevation of the lower nappe at outflow section, and additional two internal boundary conditions (atmospheric bed pressure and known elevation of the lower nappe) at the brink section, it is required to determine the upper flow surface profile, ACE, and the lower nappe profile, DF. It is also required to compute the pressure distribution at a vertical section and bed pressure profile upstream of the end section as part of the solution. For this purpose,

the computational domain of the flow problem is discretized into equal size steps in  $x$  as shown in Figure 1.

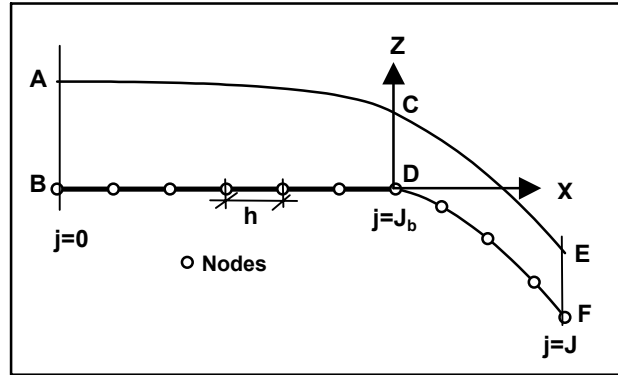


Figure 1 Computational domain for a free overfall problem.

### 3.2 Discretization of the Equations and Solution Procedure

A numerical solution is necessary since closed-form solutions are not available for these nonlinear differential equations. The finite difference approximations are used to discretise the above flow equations. This formulation is very simple to code and extensively used to solve linear or nonlinear differential equations. For discretization purpose, eqs. 1 and 3 can be represented by a simple general equation as

$$\frac{dH^3}{dx^3} + \xi_0 \frac{dH^2}{dx^2} + \xi_1 \frac{dH}{dx} + \xi_2 = 0, \tag{6}$$

where  $\xi_0$ ,  $\xi_1$  and  $\xi_2$  are the nonlinear coefficients associated with the equations. Higher-order finite difference approximations are employed here to replace the derivative terms in these equations in order to reduce the truncation errors introduced in the formulation due to the finite difference quotients (see e.g., Fletcher (1991)). The upwind finite difference approximations (Bickley (1941)) for derivatives at node  $j$  in terms of the nodal values at  $j - 2$ ,  $j - 1$ ,  $j$  and  $j + 1$  are introduced into eq. 6 in places of the derivatives. After simplifying the resulting expression and assembling similar terms together, the equivalent finite difference equation reads as

$$H_{j-2}(-6 + \xi_{1,j}h^2) + H_{j-1}(18 + 6\xi_{0,j}h - 6\xi_{1,j}h^2) + H_j(-18 - 12\xi_{0,j}h + 3\xi_{1,j}h^2) + H_{j+1}(6 + 6\xi_{0,j}h + 2\xi_{1,j}h^2) + 6\xi_{2,j}h^3 = 0, \tag{7}$$

where  $h$  is the size of the step. Since the value of the nodal point at  $j = 0$  is known, the value of the imaginary node at  $j = -1$  can be determined from the estimated water surface slope,  $S_H$ , at the inflow section. Using a similar discretization equation for the water surface slope at inflow section and the expanded form of eq. 7 at  $j = 0$ , the explicit expression for the nodal value at  $j = -1$  in terms of values of the nodal point 0 and 1 is

$$H_{-1} = \left( \frac{-1}{\Omega + 6\Pi} \right) \left( H_1\theta + H_0\Psi + \Pi(6hS_H - 3H_0 - 2H_1) + 6\xi_{2,0}h^3 \right), \quad (8)$$

where:  $\theta = 6 + 6\xi_{0,0}h + 2\xi_{1,0}h^2$ ;  $\Psi = -18 - 12\xi_{0,0}h + 3\xi_{1,0}h^2$ ;  $\Omega = 18 + 6\xi_{0,0}h - 6\xi_{1,0}h^2$ ;  $\Pi = -6 + \xi_{1,0}h^2$ .

The complete simulation of the flow profile of this problem requires the application of both the pressure and flow profile equations. To simplify the numerical simulation procedures, the contribution of the bed slope squared term in eq. 2 is neglected. Therefore, the bed pressure equations can be discretized in a general form as the flow profile equations but  $\omega_0 = 1.0$  for the BTML model. For the free jet portion of this flow, the pressure at the underside of the nappe is atmospheric. Using this condition, the discretized equation for the elevation of the lower nappe of the jet,  $Z_b$ , from the pressure equation reads as

$$Z_{b,j-1} - 2Z_{b,j} + Z_{b,j+1} = -\frac{h^2}{\omega_0} \left( \frac{gH_j^2}{\beta q^2} + \frac{1}{2h^2} (H_{j-1} - 2H_j + H_{j+1}) \right). \quad (9)$$

At nodal point  $j = J$ , the elevation of the lower nappe is specified as an outflow boundary condition and at  $j = J_b$  the elevation of this nappe is the same as the elevation of the bed. For the simulation of the upper flow profile, an internal boundary condition (atmospheric bed pressure) is imposed at the brink section. Thus, the discretized equation for part of the curvature term of the upper nappe profile at this section from the pressure equation becomes

$$H_{j-1} - 2H_j + H_{j+1} = -2h^2 \left( \frac{2gH_j^2}{\beta q^2} + 2\omega_0 \left( \frac{d^2 Z_b}{dx^2} \right)_j \right). \quad (10)$$

The use of eq. 7 at nodal point  $j = J$  for the upper nappe profile will introduce an unknown nodal value external to the computational domain. Using the backward difference approximations in terms of nodal points  $J, J-1, J-2 \dots$  for the derivative terms in eq. 6, the finite difference equation at the outflow section after simplifying the resulting expression becomes

$$H_{j-4} (36 + 22\xi_{0,j}h + 6\xi_{1,j}h^2) + H_{j-3} (-168 - 112\xi_{0,j}h - 32\xi_{1,j}h^2) + H_{j-2} (288 + 228\xi_{0,j}h + 72\xi_{1,j}h^2) + H_{j-1} (-216 - 208\xi_{0,j}h - 96\xi_{1,j}h^2) + H_j (60 + 70\xi_{0,j}h + 50\xi_{1,j}h^2) + 24\xi_{2,j}h^3 = 0. \quad (11)$$

The solution of the nonlinear flow equation based on a boundary value technique requires an initial estimate of the position of the free surface profile. This makes the solution of the flow problems relatively more difficult due to the fact that the location of the free surface profile is not known a priori. Generally, such problems must be solved by iterative methods, which proceed from an assumed initial free surface position. Convergence of the iteration procedure to a final profile that satisfies the boundary conditions may be dependent to some extent on the choice of the initial flow surface profile. In this work the Bernoulli and continuity equations are employed to obtain the initial upper flow surface profile for commencing the iteration solution. Also, the initial lower nappe profile is taken as a horizontal continuation of the channel bed. Since the curvature of the fixed bed is known, eqs. 7, 8, 10 and 11, with the inflow boundary conditions are solved numerically to

simulate the upper flow surface profile. To predict the lower nappe flow profile, eq. 9 together with the specified two boundary conditions is solved using similar technique. In each iteration process the derivatives of the lower nappe profile are computed numerically. The application of these equivalent finite difference equations at different nodal points within the solution domain results a sparse system of nonlinear algebraic equations. These equations with the appropriate boundary values at the specified sections are solved implicitly using a Newton-Raphson iterative scheme with a numerical Jacobian matrix. The convergence of the solution is assessed using the following criterion:

$$\sum_{j=1}^m |\delta H_j| \leq \text{tolerance},$$

where  $\delta H_j$  is the correction depth to the solution of the nodal point  $j$  at any stage in the iteration;  $m$  is the total number of nodes in the solution domain excluding nodes having known values. In this study, a tolerance of  $10^{-6}$  is used for the convergence of the numerical solution.

For the solution of the pressure equations, a similar finite difference approximation is inserted into eqs. 2 and 4 to discretise the derivative term in the equations. Since the nodal flow depth values are known from the solution of the flow profile equations, these discretized equations yield the bed pressure (for  $z = Z_b$ , where  $Z_b$  is channel bed elevation) at different nodal points.

## 4. RESULTS AND DISCUSSION

The one-dimensional numerical models presented in the previous sections are now used for simulating steady: i) flow in a free overfall with subcritical approaching flow; and ii) transcritical flow over short-crested trapezoidal profile weirs. Since the experiments for both cases were performed in Plexiglass laboratory flumes, a smooth boundary resistance law was used to estimate the friction slope for the models. For computational simplicity,  $\beta$  is assumed as unity in both models. All numerical results presented here were independent of the effect of spatial step size.

### 4.1 Free Overfall

In this work, the Rajaratnam and Muralidhar (1968) experimental data for free overfall in a rectangular channel were used for the verification of the model results. The computed flow surface profiles for subcritical approaching flow is compared with the experimental results in Figure 2. Upstream of the brink section, the results of both models agree well with the experimental data. Although the observation was taken for short length of the flow domain, the BTMU model simulates the upper nappe profile of the jet more accurately than the BTML model. The BTML model result starts to deviate from the measured data for this part and shows very steep water surface slope at the brink section. For this flow situation, the brink depth is an important parameter for estimating the flow rate. This depth is predicted accurately by the BTMU model with an error of less than 3%. Figure 3 shows the bed pressure profile upstream of the end section. In this figure the non-dimensional bed pressure at any section,  $p_b / p_0$  ( $p_b$  = bed pressure,  $p_0 = \rho g H$ ) is shown versus the normalized distance from the brink,  $x / H$ . As can be seen from this figure, the predicted results compared very well with the experimental data. Both models predict similar bed pressure profiles.

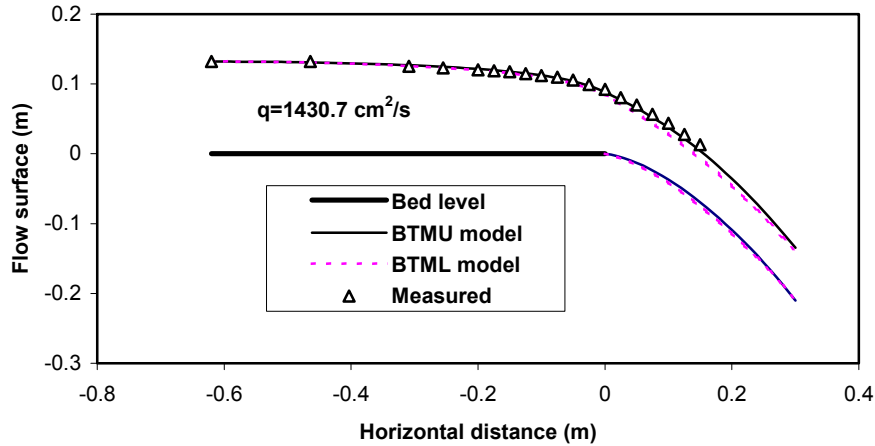


Figure 2 Flow surface profile in a free overfall with subcritical upstream flow.

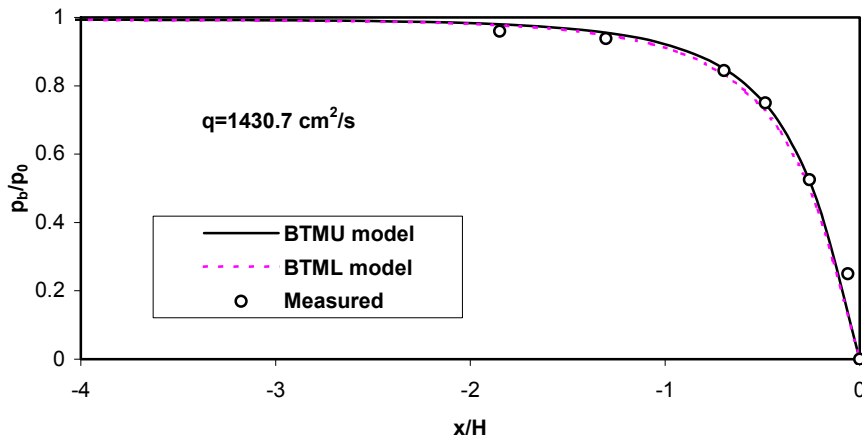


Figure 3 Bed pressure profile in a free overfall with subcritical upstream flow.

Figure 4 plots the non-dimensional pressure distribution upstream of the fall,  $p/p_0$  ( $p$  = pressure at height,  $h_s$ , above the bed) versus the non-dimensional height above the bed,  $h_s/H$ . In this figure, the computed pressure distributions are compared with the experimental results. It can be seen from this figure that the result of the BTMU model shows internal atmospheric pressure at the brink section due to the pre-assumed constant centrifugal term at a vertical section. Contrary to this, the BTML model predicts the maximum pressure at the end section accurately. However, the numerical solution indicates some deviation for the location of the maximum pressure. This difference between the numerical and experimental results is about 27% of  $H$ . In general, the prediction of the pressure distribution profile using the BTML model is satisfactory and follows a similar pattern with the observed values. Also, this model predicts the pressure distributions more accurately at vertical sections, 5.72 cm and 11.43 cm to the left of the free overfall, where the flow has considerable streamline curvature. At a distance of 17.15 cm from the end section the curvature of streamline is negligible; both models provide similar results which agree very well with the experimental data. This comparison suggests that a higher-order pressure equation should be used to simulate accurately the pressure distribution of a flow with pronounced curvature of streamlines.

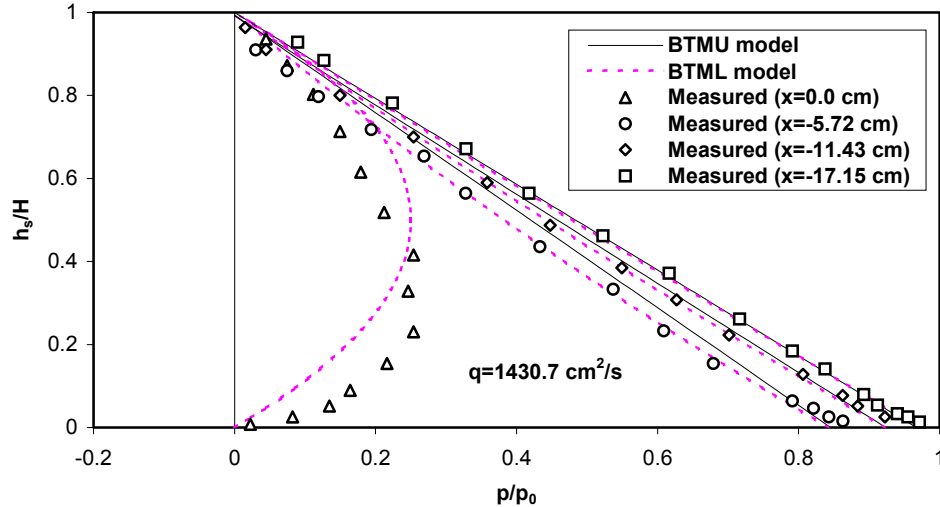


Figure 4 Pressure profiles in a free overfall at different sections.

#### 4.2 Flow Over Short-crested Trapezoidal Profile Weirs

Experiments on flow over trapezoidal profile weirs were conducted for validating the results of the models. Details of the experimental system can be found in Zerihun and Fenton (2004). To assess the effect of the streamline curvature on the solution of the models, transcritical flow over trapezoidal profile weirs with different  $H_0/L_w$  ( $H_0$  = total energy head over the weir crest,  $L_w$  = weir crest length) values were considered. The computed flow surface and bed pressure profiles for this flow situation are compared with experimental results in Figures 5 and 6. The BTMU and BTML models solutions for flow surface profile show excellent agreement with the measured data. Both models predict similar flow surface profiles with steep flow surface slope on the crest of the weir. A minor discrepancy between the results of the two models for bed pressure profiles can be seen from these figures. In general, the overall qualities of the numerical solutions of the bed pressure are good and show good agreement with the experimental data.

The comparisons for the above two flow situations indicate that the assumed shapes for the distribution of the centrifugal term has little effect on the flow surface profile solutions of the models.

### 5. CONCLUSIONS

Two one-dimensional Boussinesq-type momentum equation models were investigated for simulating free overfall in a rectangular channel and transcritical flow over short-crested trapezoidal profile weirs. Uniform and linear distribution shapes for the variation of the centrifugal term were used to develop the equations. Finite difference approximations were employed to discretise the flow equations. The resulting nonlinear algebraic equations were solved using the Newton-Raphson technique with a numerical Jacobian matrix. The comparison result for flow surface profiles shows that the BTMU model provides better agreement with the measurement than the BTML model for the simulation of free overfall flow problem. For the transcritical weir flow situation, the agreement between the experimental and numerical results is good and no significance differences are observed between the computational results of the two models for the entire flow region. For both cases of the flow problems, the dynamic pressure simulation of the BTML model is much better than the BTMU

model particularly in the flow region where the effect of non-hydrostatic pressure distribution is predominant. This numerical experiment demonstrates that the pressure profile results are very sensitive to the applied approximations for the variation of the centrifugal term, but the flow profile solutions are little affected by these approximations.

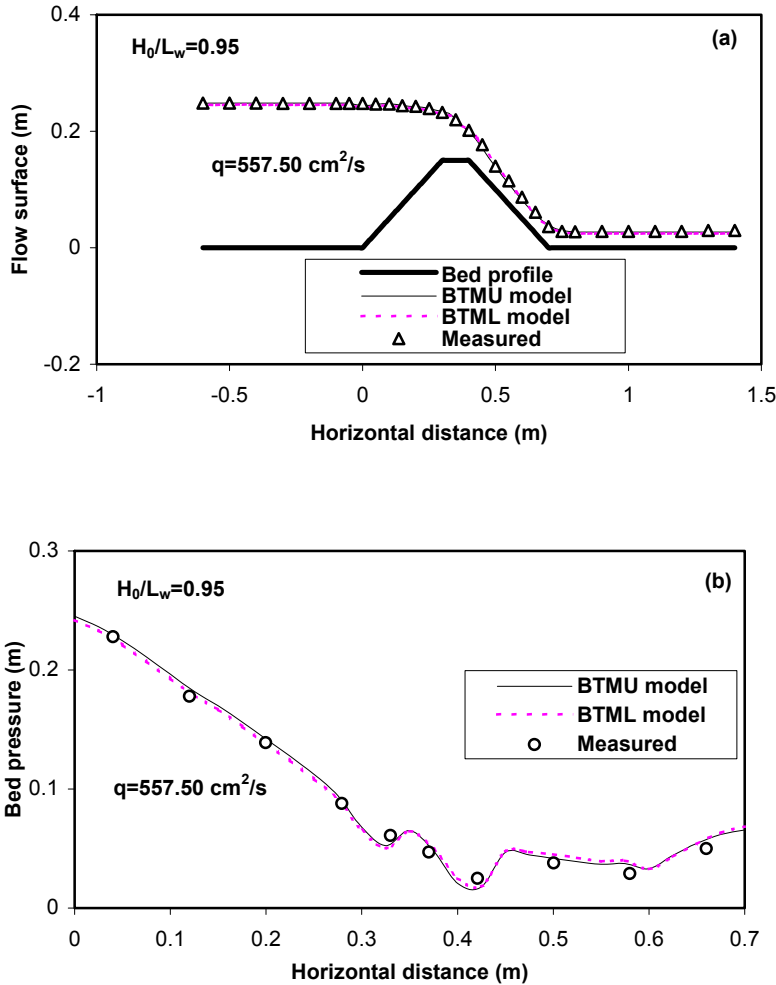
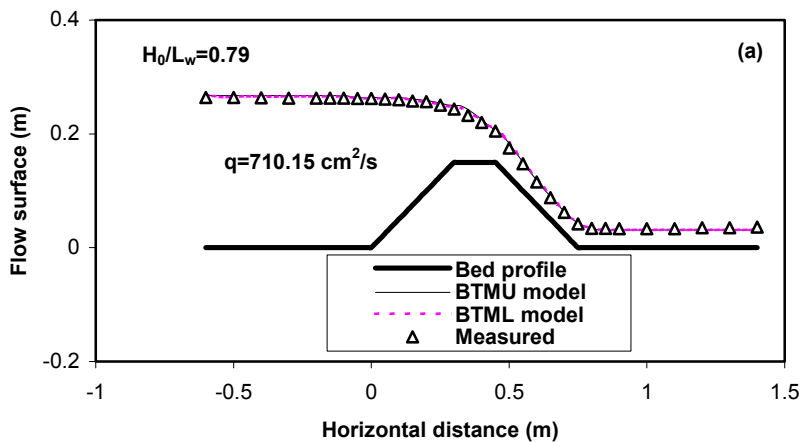


Figure 5 Flow surface and bed pressure profiles for free flow situation ( $L_w = 10$  cm).



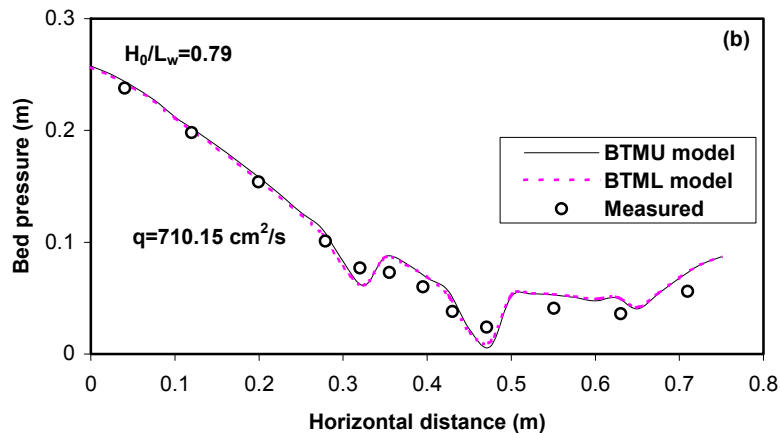


Figure 6 Flow surface and bed pressure profiles for free flow situation ( $L_w=15$  cm).

## REFERENCES

- Bickley, W. G. (1941). "Formulae for Numerical Differentiation", *Math. Gaz.* Vol. 25, pp. 19-27.
- Boussinesq, J. (1877). "Essai Sur la Théorie des Eaux Courantes", *Mémoires Présentés par Divers Savants à l'Académie des Sciences, Paris*, Vol. 23, No.1, pp.1-680.
- Dressler, R. F. (1978). "New Nonlinear Shallow Flow Equations with Curvature", *Journal of Hydraulic Research*, Vol. 16, No.3, pp. 205-220.
- Fenton, J. D. (1996). "Channel Flow Over Curved Boundaries and a New Hydraulic Theory", *Proceedings of the 10<sup>th</sup> Congress, APD-IAHR, Langkawi, Malaysia*, Vol. 2, pp. 266-273.
- Fletcher, C. A. J. (1991), *Computational Techniques for Fluid Dynamics 1*, Springer-Verlag Berlin Heidelberg, Germany.
- Hager, W. H. and Hutter, K. (1984). "Approximate Treatment of Plane Channel Flow", *Acta Mechanica*, Vol. 51, pp. 31-48.
- Hager, W. H. (1985). "Equation of Plane, Moderately Curved Open Channel Flows", *Journal of Hydraulic Engineering, ASCE*, Vol. 111, No. 3, pp. 541-546.
- Henderson, F. M. (1966). *Open Channel Flow*, Macmillan, New York.
- Khan, A. A. and Steffler, P. M. (1996a). "Vertically Averaged and Moment Equations Model for Flow Over Curved Beds", *Journal of Hydraulic Engineering, ASCE*, Vol. 122, No. 1, pp. 3-9.
- Khan, A. A. and Steffler, P. M. (1996b). "Modelling Overfalls Using Vertically Averaged and Moment Equations", *Journal of Hydraulic Engineering, ASCE*, Vol.122, No. 7, pp. 397-402.
- Matthew, G. D. (1991). "Higher Order, One-dimensional Equations of Potential Flow in Open Channels", *Proceedings of the Institution of Civil Engineers*, Vol. 91, pp. 187-201.
- Rajaratnam, N., and Muralidhar, D. (1968). "Characteristics of the Rectangular Free Overfall", *Journal of Hydraulic Research*, Vol. 6, No. 3, pp. 233-258.
- Steffler, P. M., and Jin, Y. (1993). "Depth Averaged and Moment Equations for Moderately Shallow Free Surface Flow", *Journal of Hydraulic Research*, Vol. 31, No. 1, pp. 5-17.
- Zerihun, Y. T. and Fenton, J. D. (2004). "A One-dimensional Flow Model for Flow Over Trapezoidal Profile Weirs", *Proceedings of the 6<sup>th</sup> International Conference on Hydro-science and Engineering*, Brisbane, May 30-June 3, CD-ROM.